Received: 11 May 2017 | Revised: 16 March 2018 | Accepted: 26 March 2018

DOI: 10.1111/ter.12336

PAPER

WILEY Terra Nova

Tectonothermal history of the Holy Cross Mountains (Poland) in the light of low-temperature thermochronology

Dariusz Botor[1] | Aneta A. Anczkiewicz[2] | István Dunkl[3] | Jan Golonka[1] | Mariusz Paszkowski[2] | Stanisław Mazur[2]

[1]Faculty of Geology, Geophysics and Environmental Protection, AGH University of Science and Technology, Kraków, Poland

[2]Institute of Geological Sciences, Polish Academy of Sciences, Kraków, Poland

[3]Sedimentology and Environmental Geology, Geoscience Center, University of Göttingen, Göttingen, Germany

Correspondence
Dariusz Botor, Faculty of Geology, Geophysics and Environmental Protection, AGH University of Science and Technology, Kraków, Poland.
Email: botor@agh.edu.pl

Funding information
Polish National Centre for Research and Development (NCRD) under the Blue Gas – Polish Shale Gas Program, Grant/Award Number: BG1/GAZGEOLMOD/13, 17.17.866660; National Science Centre, Grant/Award Number: UMO-2012/05/B/ST10/00521

Abstract

The low-temperature thermal history of the Holy Cross Mountains (HCM) is investigated by apatite fission track and apatite and zircon (U–Th)/He thermochronology. Our results provide constraints on the deformation history of Palaeozoic basement rocks in the transition area from Precambrian to Palaeozoic Europe that are exposed from beneath Permian–Mesozoic sediments within the HCM. Late to post-Variscan cooling of the Palaeozoic strata from maximum temperatures is shown to be a major feature of the HCM. This cooling likely followed a heating event related to burial and/or hot fluid circulation along the Holy Cross Fault in the late Carboniferous. The central part of the HCM shows a rapid cooling event caused by tectonic inversion, which started in the Late Cretaceous. However, this event was less pronounced in the western margin of the HCM, where slow cooling continued throughout the Mesozoic with only minor acceleration of the cooling rate since the latest Cretaceous.

1 | INTRODUCTION

The Holy Cross Mountains (HCM) are a solitary massif built of polydeformed Cambrian–Carboniferous sediments (Figure 1) that were exhumed from beneath a Permian–Mesozoic cover during Late Cretaceous–Palaeocene inversion of the Polish Basin (Krzywiec, 2009; Krzywiec, Gutowski, Walaszczyk, Wróbel, & Wybraniec, 2009; Lamarche, Lewandowski, Mansy, & Szulczewski, 2003; Lamarche et al., 1999; Lamarche, Scheck, et al., 2003; Mazur, Scheck-Wenderoth, & Krzywiec, 2005; Scheck-Wenderoth, Krzywiec, Zülke, Maystrenko, & Frizheim, 2008). This massif provides a unique insight into the tectonic history of the pre-Permian basement that underlies the Polish Basin next to the Teisseyre–Tornquist Zone and the margin of the Precambrian East European Platform (Figure 1; e.g. Berthelsen, 1992; Dadlez, Kowalczewski, & Znosko, 1994; Lamarche et al., 1999; Nawrocki et al., 2007). The Palaeozoic massif of the HCM emerges on both sides of the boundary between the Łysogóry and Małopolska Blocks, separated by the Holy Cross Fault (HCF; Figure 1).

The Palaeozoic and Mesozoic thermal history of the HCM was controlled by intervening episodes of subsidence, burial and inversion, but is still not sufficiently understood. There is no consensus on the tectonothermal evolution of the HCM and several contradicting models have been proposed. Most authors (Bełka, 1990; Marynowski, 1997, 1999; Marynowski, Salamon, & Narkiewicz, 2002; Naglik, Toboła, Natkaniec-Nowak, Luptáková, & Milovská, 2016; Narkiewicz, 2017; Narkiewicz, Resak, Littke, & Marynowski, 2010; Smolarek, Marynowski, Spunda, & Trela, 2014) argue for an elevated Variscan (late Carboniferous to early Permian) heat flow, which significantly exceeded the current low values (Szewczyk & Gientka, 2009). However, Poprawa, Żywiecki, and Grotek (2005) proposed that thermal maturity of organic matter in the Devonian to Jurassic sedimentary successions was achieved during Late Jurassic or Late Cretaceous burial that was characterized by constant heat flow equal

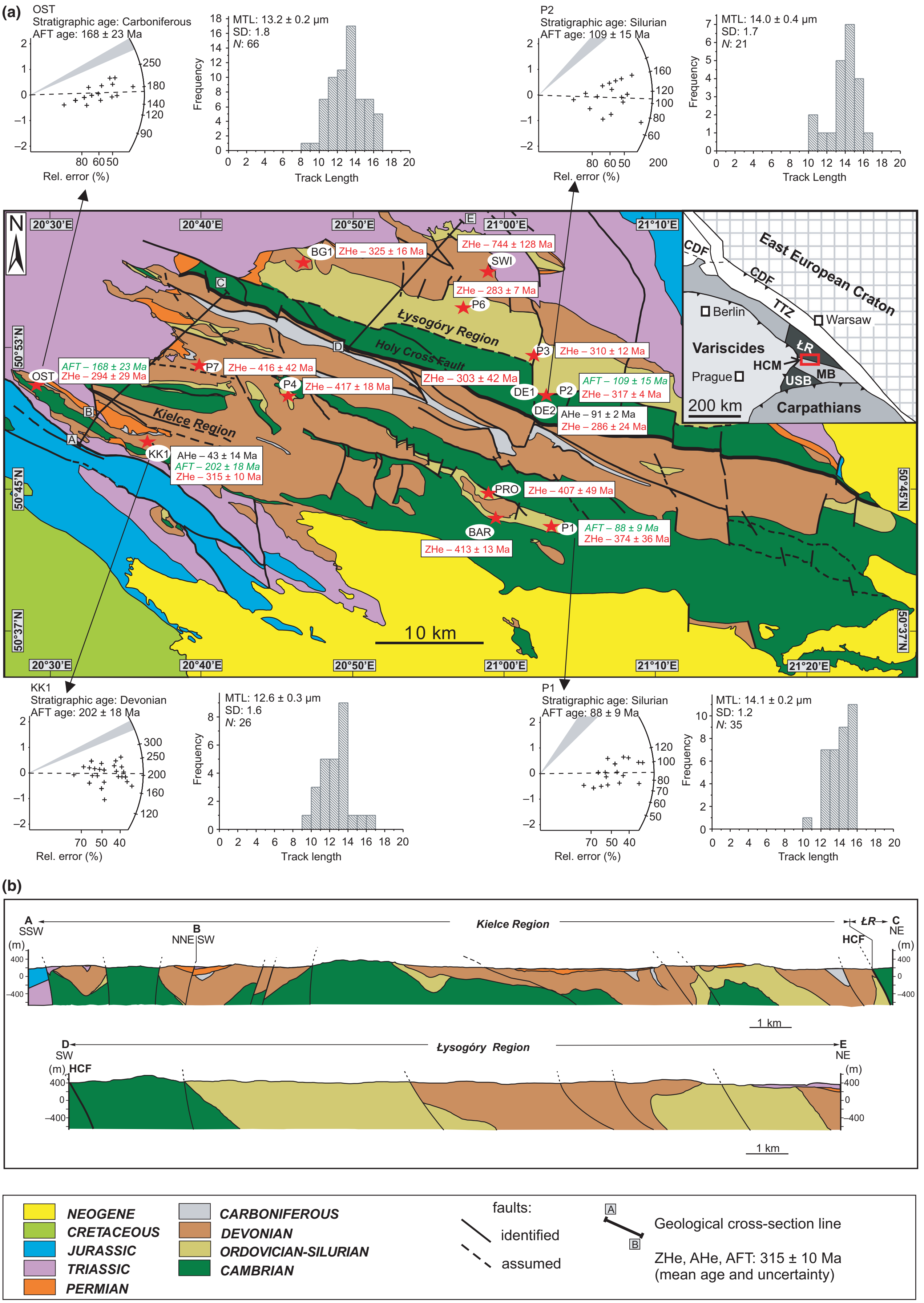
(a)
OST
Stratigraphic age: Carboniferous
AFT age: 168 ± 23 Ma
Rel. error (%)
MTL: 13.2 ± 0.2 μm
SD: 1.8
N: 66
Frequency
Track Length
P2
Stratigraphic age: Silurian
AFT age: 109 ± 15 Ma
Rel. error (%)
MTL: 14.0 ± 0.4 μm
SD: 1.7
N: 21
Frequency
Track Length
20°30'E
20°40'E
20°50'E
21°00'E
21°10'E
21°20'E
50°53'N
50°45'N
50°37'N
BG1 ZHe – 325 ± 16 Ma
ZHe – 744 ± 128 Ma
SWI
ZHe – 283 ± 7 Ma
P6
Łysogóry Region
Holy Cross Fault
P3 ZHe – 310 ± 12 Ma
AFT – 168 ± 23 Ma
OST ZHe – 294 ± 29 Ma
P7 ZHe – 416 ± 42 Ma
P4 ZHe – 417 ± 18 Ma
ZHe – 303 ± 42 Ma
DE1
P2 AFT – 109 ± 15 Ma
ZHe – 317 ± 4 Ma
DE2 AHe – 91 ± 2 Ma
ZHe – 286 ± 24 Ma
Kielce Region
KK1 AHe – 43 ± 14 Ma
AFT – 202 ± 18 Ma
ZHe – 315 ± 10 Ma
PRO ZHe – 407 ± 49 Ma
BAR
P1 AFT – 88 ± 9 Ma
ZHe – 374 ± 36 Ma
ZHe – 413 ± 13 Ma
10 km
East European Craton
CDF
TTZ
Berlin
Warsaw
Variscides
ŁR
HCM
MB
Prague
USB
200 km
Carpathians
KK1
Stratigraphic age: Devonian
AFT age: 202 ± 18 Ma
Rel. error (%)
MTL: 12.6 ± 0.3 μm
SD: 1.6
N: 26
Frequency
Track length
P1
Stratigraphic age: Silurian
AFT age: 88 ± 9 Ma
Rel. error (%)
MTL: 14.1 ± 0.2 μm
SD: 1.2
N: 35
Frequency
Track length
(b)
A SSW
B NNE SW
Kielce Region
ŁR
C NE
HCF
(m)
1 km
D SW
Łysogóry Region
E NE
HCF
1 km
NEOGENE
CRETACEOUS
JURASSIC
TRIASSIC
PERMIAN
CARBONIFEROUS
DEVONIAN
ORDOVICIAN-SILURIAN
CAMBRIAN
faults:
identified
assumed
Geological cross-section line
ZHe, AHe, AFT: 315 ± 10 Ma
(mean age and uncertainty)

FIGURE 1 (a) Simplified geological map of the Holy Cross Mountains (compiled from various sources including Czarnocki, 1950; Konon, 2007) with thermochronological data and (b) cross-sections (A–B–C and D–E). ZHe, mean zircon helium age; AHe, mean apatite helium age; AFT, apatite fission track central age; all errors are 1σ; MTL, mean track length; *SD*, standard deviation; *N*, number of confined horizontal tracks; analytical details are given in the Supporting Information (Tables SI 1–SI 3). Inset in the upper right corner shows regional tectonic elements (CDF, Caledonian Front; MB, Małopolska Block; ŁR, Łysogóry Region; USB, Upper Silesia Block; TTZ, Teisseyre–Tornquist Zone; HCM, Holy Cross Mountains). Red rectangle in the inset map marks the study area and outline of the geological map

to the recent one (Szewczyk & Gientka, 2009). They concluded that no elevated Variscan heat flow was necessary to explain the observed maturity in the Palaeozoic formations. Schito et al. (2017) presented burial and thermal history models, assuming very low constant heat flow during the Palaeozoic to Jurassic that subsequently increased up to the present-day values from the Early Cretaceous onwards with maximum palaeotemperatures reached in the Late Cretaceous. Most authors agree about a key role of the HCF in controlling the Variscan thermal regime within the region (Bełka, 1990; Marynowski, 1999; Poprawa et al., 2005) and enhancing Carboniferous–Permian advective heat flow by fluid migration (Naglik et al., 2016; Narkiewicz et al., 2010; Poprawa et al., 2005). In the HCM, burial and exhumation events of different magnitudes can be related to the HCF polyphase activity. Particularly, Variscan deformation in the late Carboniferous (e.g. Lamarche, Lewandowski, et al., 2003; Narkiewicz, 2007) was potentially capable of generating a tectonic overburden which might have caused a temperature increase and affected thermal maturity of organic matter.

The aim of our study was to reveal for the first time the thermal history of the HCM in the temperature range below 200°C by applying apatite fission track (AFT) and apatite and zircon (U–Th)/He dating techniques.

2 | GEOLOGICAL SETTING

Lower Cambrian–lower Carboniferous sediments form the Palaeozoic massif of the HCM that is discordantly covered by upper Permian–Upper Cretaceous sediments forming a margin in the N, W and SW of the Palaeozoic core. The core and its margin are jointly overlain by a transgressive Miocene fill of the Carpathian foredeep basin that covers the Palaeozoic inlier of the HCM from the S and SE (Figure 1). The structure of the HCM was shaped by several episodes of tectonic shortening in the late Cambrian, latest Silurian–earliest Devonian (Caledonian), late Carboniferous (Variscan) and Late Cretaceous–Palaeocene (Alpine) interrupted by long periods of basin-forming subsidence (e.g. Czarnocki, 1919; Gągała, 2015; Konon, 2006, 2007; Kowalczewski, Jaworowski, & Kuleta, 1998; Kutek & Głazek, 1972; Lamarche, Lewandowski, et al., 2003; Lamarche et al., 1999; Lamarche, Scheck, et al., 2003; Szaniawski, Konon, Grabowski, & Schnabl, 2011; Znosko, 1996).

The stratigraphy of the Palaeozoic core of the HCM shows similarities to both the East European Platform in the north and the Małopolska Block in the south. The part of the HCM north of the HCF, referred to as the Łysogóry Region after Czarnocki (1936) (Figures 1 and 2), contains a ~7 km thick, nearly continuous middle Cambrian–Upper Devonian stratigraphic section (e.g. Jaworowski & Sikorska, 2006; Kozłowski, 2003). The part S of the HCF, known as the Kielce Region (Figure 1; Czarnocki, 1936), includes a thinner and less complete lower Cambrian–lower Carboniferous stratigraphic section (Figure 2; e.g. Modliński & Szymański, 2001; Nawrocki et al., 2007; Szulczewski, 1995). The HCF, separating the Łysogóry and Kielce Regions, was variously interpreted as a flower structure (Lamarche, Lewandowski, et al., 2003), a strike-slip duplex (Mastella & Mizerski, 2002), a series of vertical-axis rotated blocks (Konon, 2007) or a thin-skinned thrust (Czarnocki, 1919, 1950; Gągała, 2015; Stupnicka, 1988, 1992).

Variscan deformation of the HCM is manifested by the occurrence of Carboniferous folds and thrusts (e.g. Konon, 2006; Lamarche, Lewandowski, et al., 2003; Mizerski, 2004) as well as the presence of a thin-skinned fold-and-thrust belt encroaching onto the East European Craton directly SE of the HCM (Krzywiec, Gągała, et al., 2017; Krzywiec, Mazur, et al., 2017). The kinematic mechanism of the Variscan folding inside the HCM was interpreted as a multi-detachment buckling by Konon (2006), who proposed several décollements dispersed throughout the Palaeozoic strata. After Variscan shortening and inversion, revealed by a major base-Permian unconformity (e.g. Lamarche, Lewandowski, et al., 2003; Narkiewicz et al., 2010), the HCM underwent a prolonged Mesozoic subsidence as part of the Polish Basin floor (e.g. Dadlez, Narkiewicz, Stephenson, Visser, & Van Wees, 1995; Kutek, 2001; Kutek & Głazek, 1972; Lamarche, Lewandowski, et al., 2003; Narkiewicz et al., 2010). The eastern and central parts of the HCM were located in the axial zone of the Mid-Polish Trough representing a main Permian–Mesozoic depocentre (e.g. Dadlez et al., 1995; Kutek, 2001; Kutek & Głazek, 1972; Lamarche, Lewandowski, et al., 2003). The HCM were exhumed from beneath a Permian–Mesozoic cover during the Late Cretaceous–Palaeocene Alpine inversion of the Polish Basin, when the Mid-Polish Trough was inverted into the Mid-Polish Swell with its axis ascending SE-ward (Krzywiec, 2002; Krzywiec et al., 2009; Lamarche, Lewandowski, et al., 2003; Lamarche, Scheck, et al., 2003; Mazur et al., 2005; Scheck-Wenderoth et al., 2008).

3 | SAMPLES AND METHODS

Lower Ordovician to lower Carboniferous sandstone and bentonite samples were collected from surface outcrops in the HCM. We applied three low-temperature thermochronology methods: AFT, (U–Th)/He on zircon (ZHe) and apatite (AHe). Thermal histories were

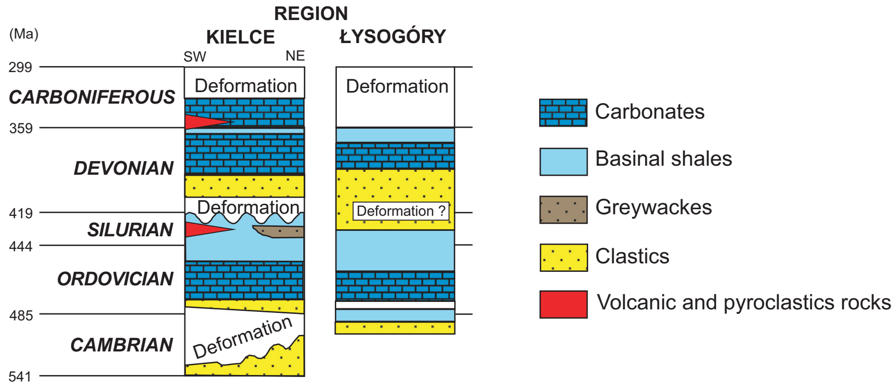

FIGURE 2 Synthetic stratigraphic columns of the Palaeozoic for the Kielce and Łysogóry Regions of the Holy Cross Mountains (compiled from various sources including Czarnocki, 1950; Kozłowski, 2008; Kozłowski, Domańska-Siuda, & Nawrocki, 2014; Malec, Kuleta, & Migaszewski, 2016; Narkiewicz, 2007; Narkiewicz et al., 2010; Szulczewski, 1995; Szulczewski, Bełka, & Skompski, 1996)

modelled using the HeFTy software (Ketcham, 2005), applying a multikinetic apatite annealing model (Ketcham, Carter, Donelick, Barbarand, & Hurford, 2007a, 2007b) using Dpar as kinetic parameter. Details of each method are included in the Supporting Information. Chronostratigraphic subdivisions and absolute ages refer to Gradstein, Ogg, and Hilgen (2012) throughout the text.

4 | RESULTS

ZHe dating results for 14 samples are listed in Tables 1 and SI 1. A few grains yielded ages that are statistical outliers, probably due to submicroscopic inclusions or other imperfections. These grains were excluded from the calculation of mean ZHe ages. In the Łysogóry Region, the Silurian and Devonian samples gave mean ages between 325 and 283 Ma (Figure 1). Sample SW1, however, is distinctly older (744 Ma) than its depositional age and represents preserved provenances signal. All other ZHe ages are younger than the stratigraphic age and thus considered totally reset and representing Variscan cooling ages. In the Kielce Region, Ordovician and Silurian samples have ZHe ages from 417 to 407 Ma, with one younger age of 374 Ma (P1). These ages are thought to be partially reset during a Variscan heating event. The ZHe age of sample KK1 (315 Ma) is thought to be entirely reset since all the single grain ages are younger than their stratigraphic age and narrowly clustered. However, the Viséan OST sample has a mean ZHe age of 294 Ma, based on three single grain ages which scatter from 352 to 256 Ma, suggesting no full reset (Tables 1 and SI 1).

AFT ages for four samples are significantly younger than the stratigraphic age (Tables 1 and SI 2). Mean track lengths range from 12.6 to 14.1 μm, and track length distributions are unimodal with relatively narrow standard deviations (1.2–1.8 μm; Figure 1; Table SI 2). The samples are considered to have undergone full annealing. Mean Dpars range between 2.4 and 3.0 μm, indicating increased annealing resistance with respect to fluorapatite (Donelick, O'Sullivan, & Ketcham, 2005; Ketcham et al., 2007a, 2007b). In the Łysogóry Region, sample P2 gave a Cretaceous cooling age (109 Ma), while three samples (P1, OST and KK1) in the Kielce Region yielded ages of 88, 168 and 202 Ma.

Samples DE2 (Łysogóry Region) and KK1 (Kielce Region) yielded apatite crystals suitable for AHe thermochronology with average AHe ages of 91 Ma and 43 Ma respectively (Tables 1 and SI 3). These ages show continued Cretaceous and Palaeogene cooling.

Thermal histories were modelled for samples KK1, P1 and P2 (in combination with the AHe age of DE2 from the same locality). The objectives of the modelling were (1) to indirectly estimate maximum temperatures in the late Palaeozoic that can be approximated by the ZHe data and (2) to constrain the cooling path by ZHe, AFT and AHe data. The starting point of the time–temperature (t–T) path for the studied samples was set at T = 25–20°C in the time interval that corresponds to the range of the stratigraphic ages.

A late Palaeozoic Variscan heating event occurred with maximum temperatures reaching c. 130 and 180°C in the Kielce and Łysogóry Regions respectively (Figure 3). Post-Variscan cooling followed shortly after and resulted in exhumation of the sediments into the AFT annealing zone by the late Permian. The models for samples P2/DE2 and P1 show a gradual temperature increase up to 120°C in the Mesozoic and a thermal plateau at 100–110°C respectively (Figure 3). In contrast, thermal modelling for sample KK1, from the western Kielce Region, proposes ongoing cooling throughout the Mesozoic with only minor acceleration in the Late Cretaceous (Figure 3a). The other thermal modelling suggests rapid exhumation in the Late Cretaceous, but reduced cooling in the Cenozoic (Figure 3b, c). For modelling details, see the Supporting Information.

5 | DISCUSSION

The modelling results are consistent with the assumption of moderate to elevated Variscan heat flow on both sides of the HCF. The whole Cambrian–lower Carboniferous succession was heated in the Carboniferous and subsequent cooling commenced in the latest Carboniferous and endured into the Permian. Previous studies showed that the maturity of Devonian and lower Carboniferous rocks

TABLE 1 Sample locations and thermochronological data from the Holy Cross Mountains. For analytical details, see Tables SI 1–SI 3

Sample code	Locality description	Co-ordinates		Elevation (m)	Lithology	Stratigraphic age of sample (c. numeric age, Ma)	Thermal maturity: Conodont CAI	Thermal maturity: VR (%)	Max. temp. (°C)	ZHe age (Ma) average	N	Single grain ZHe age range in sample (Ma)	SD	AFT age (Ma)	N	MTL (μm) (±SD)	AHe age (Ma) average	N
	Łysogóry Region																	
SWI	Świętomarz	50°56′43″N	21°01′31″E	253	Sandstone	Givetian (388–383)	~2[a]	0.8	100–110	744 ± 128	2	835.5–653.9	128.5					
BG1	Bukowa Góra	50°58′05″N	20°48′01″E	395	Bentonite	Emsian (408–393)		1.2[c]	140–160	325 ± 16	3	294.2–350.	28.4					
P2	Dębniak	50°50′36″N	21°05′17″E	314	Greywacke	Ludlowian (427–423)		1.3–1.6[d,e]	170–200	317 ± 4	3	326.6–311.8	7.8	109 ± 15	17	14.0 ± 1.7		
DE1	Dębniak	50°50′36″N	21°05′17″E	313	Greywacke	Ludlowian (427–423)		1.3–1.6[d,e]	170–200	303 ± 42	3	364.8–261 (556.9)	54.6					
DE2	Dębniak	50°50′36″N	21°05′17″E	313	Mudstone	Ludlowian (427–423)		1.3–1.6[d,e]	170–200	286 ± 24	3	317.0–256.8 (616.9)	42.6				91 ± 2	3
P3	Serwis	50°53′03″N	21°04′54″E	235	Greywacke	Ludlowian (427–423)		1.7[d,e]	190–210	310 ± 12	3	335.3–293.1	22.3					
P6	Dębno	50°53′35″N	21°00′01″E	256	Greywacke	Ludlowian (427–423)		1.7[d,e]	190–210	283 ± 7	3	288.7–278.3	7.3					
	Kielce Region																	
OST	Ostrówka	50°50′41″N	20°23′48″E	217	Bentonite	Viséan (347–331)		1.2	140–160	294 ± 29	3	352.5–256.4	50.8	168 ± 23	20	13.2 ± 1.8		
KK1	Kowala	50°48′02″N	20°35′03″E	235	Bentonite	Famennian (372–359)	~1.5[b]	0.53[c,f]	60–75[g]	315 ± 10	6	338.3–268.7	25.7	202 ± 18	30	12.6 ± 1.6	43 ± 14	4
P4	Niestachów	50°49′31″N	20°43′44″E	289	Greywacke	Ludlowian (427–423)		0.85[d]	100–110	417 ± 18	3	454.4–392.3	32.7					
P1	Zalesie	50°43′32″N	21°04′31″E	330	Greywacke	Ludlowian (427–423)		0.80[d,e]	100–110	374 ± 36	3	446–328.2	62.9	88 ± 9	20	14.1 ± 1.2		
BAR	Bardo	50°43′24″N	21°03′25″E	315	Bentonite	Wenlockian (433–427)		0.80[d]	100–110	413 ± 13	4	440.7–382.8	26.4					
PRO	Pragowiec	50°44′42″N	21°01′46″E	251	Bentonite	Ludlowian (427–423)		0.80[d,e]	100–110	407 ± 49	3	499.2–331.5	85.1					
P7	Białogon	50°50′41″N	20°34′23″E	351	Greywacke	Low. Ordovician (485–470)		0.85[d]	100–110	416 ± 42	3	492.3–344.7	74.0					

ZHe and AHe ages are given as unweighted average values.

N, number of measured crystals; *SD*, standard deviation; Uncertainty of the sample average ZHe and AHe ages are in 1 standard error, as (*SD*)/(*n*)1/2, where *SD*, standard deviation of the age replicates and *n*, number of age determinations. Uncertainty of the central AFT ages is $\pm 1\sigma$ error. The outlier age is in parenthesis. VR, mean vitrinite reflectance (but in lower Palaeozoic sediments, measurements are performed on organic particle, which are not true vitrinite but usually graptolites). Thermal maturity data are from adjacent outcrops (except KK1); therefore, they show approximate thermal maturity of thermochronological sites. Conodont CAI, Conodont Colour Alteration Index; Temp., estimation of maximum palaeotemperature based on Barker and Pawlewicz (1994).

[a] Narkiewicz et al. (2010).
[b] Bełka (1990).
[c] Marynowski (1999).
[d] Smolarek et al. (2014).
[e] Schito et al. (2017).
[f] Marynowski, Czechowski, and Simoneit (2001).
[g] Maximum temperature based on smectite illitization is *c*. 120–140°C (Środoń & Trela, 2012).

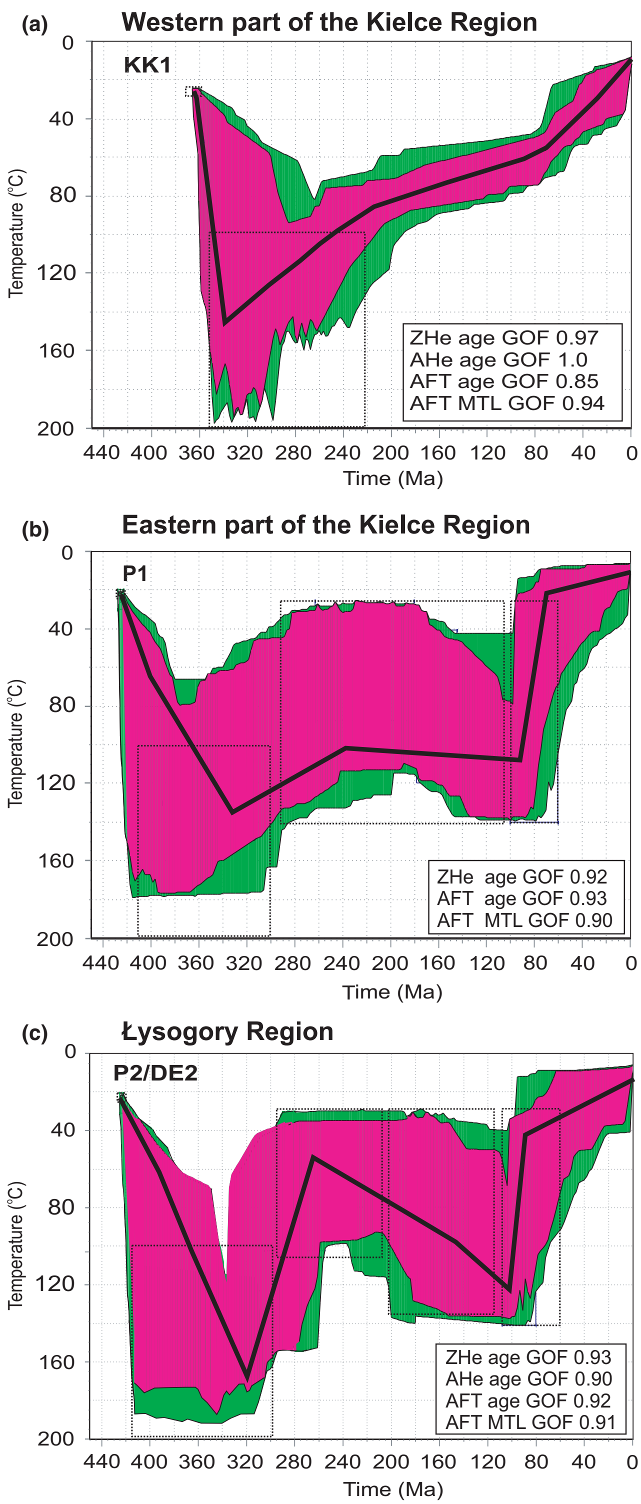

FIGURE 3 Thermal modelling results using HeFTy (Ketcham, 2005). The green range corresponds to the envelope of thermal paths with acceptable fit (goodness of fit—GOF>0.05), the purple range shows the envelope for thermal paths with good fit (GOF>0.5) (Ketcham, 2005). Bold black lines show the best fit curve, and the corresponding GOF values of each thermal dataset for this curve are listed in the lower right corner rectangle. (a) Sample KK1 from the western Kielce Region. A constraining box (dotted line) allows for maximum temperatures between 100 and to 200°C until the Early Triassic. (b) Sample P1 from the eastern Kielce Region. (c) Samples P2/DE2 from the Łysogóry Region. Constraining boxes (dotted line) allow for maximum temperatures between 100 and 200°C until the early Permian in samples P1 and P2/DE2. Additional temperature increases up to 140°C are allowed in constraining boxes during the Mesozoic. For further details, see the Supporting Information

increases towards the HCF (Bełka, 1990; Marynowski et al., 2002; Narkiewicz, 2017; Narkiewicz et al., 2010). This observation suggests large-scale fluid migration along the HCF during the late Carboniferous. Advective heat transfer by fluid migration along the HCF zone has already been postulated by Naglik et al. (2016), Narkiewicz et al. (2010) and Poprawa et al. (2005). The ZHe age of the northernmost sample SWI is not reset, suggesting that fluid penetration may have not reached the northern part of the HCM. All measured ZHe data together with the low thermal maturity of the Mesozoic sediments (Malec, 2015; Marynowski & Simoneit, 2009; Marynowski et al., 2002) contradict the occurrence of Jurassic or Cretaceous maximum palaeotemperatures as postulated by Poprawa et al. (2005) and Schito et al. (2017).

Recent seismic data image a Variscan thin-skinned thrust-and-fold belt emplaced on the SW slope of the East European Craton within the Teisseyre–Tornquist Zone, close to the HCM (Krzywiec, Gągała, et al., 2017; Krzywiec, Mazur, et al., 2017 Figure 1 inset). A Variscan compressional regime is invoked to explain the thin-skinned structuring of the pre-Permian sedimentary pile and >20 km of calculated shortening (Figure 1; Krzywiec, Gągała, et al., 2017). Hence, Variscan heating might have been caused by a combined effect of tectonic and/or sedimentary burial and elevated heat flow during the late Carboniferous.

A number of previous studies invoked late Caledonian deformation in the HCM at the Silurian–Devonian transition (e.g. Gągała, 2015; Kowalczewski et al., 1998; Znosko, 1996). This timing, constrained by angular unconformities (e.g. Gągała, 2015), agrees with average ZHe ages between 417 and 407 Ma obtained from the Ordovician and Silurian samples, except for P1 (374 Ma), in the Kielce Region. Earliest Devonian ZHe ages may indicate possible late Caledonian cooling, and no Variscan re-heating into the ZHe partial retention zone. This result is only provisional owing to the spread of single grain ages, particularly those older than deposition, and a relatively low thermal maturity of the organic matter (Bełka, 1990; Marynowski, 1999; Narkiewicz et al., 2010).

After late Variscan cooling, a temperature increase in most areas of the HCM occurred throughout the Mesozoic presumably due to sedimentary burial within the Mid-Polish Trough lasting until tectonic inversion in the Late Cretaceous (Figure 3b,c; e.g. Kutek & Głazek, 1972; Dadlez et al., 1995; Kutek, 2001; Lamarche, Lewandowski, et al., 2003). The latter was documented by the AFT data from samples P1, P2 (Figure 3b,c) and the AHe age from sample DE2 that suggest rapid cooling due to accelerated tectonic inversion of the Mid-Polish Trough, when both the Łysogóry and Kielce Regions were uplifted in the core of the Mid-Polish Swell (Krzywiec, 2002; Lamarche, Lewandowski, et al., 2003; Lamarche, Scheck, et al., 2003;

Scheck-Wenderoth et al., 2008). The onset of inversion during the early Late Cretaceous (Krzywiec et al., 2009) was associated with fast cooling underlined by a narrow time lag between AFT (P2) and AHe (DE2, same outcrop). However, in the western part of the Kielce Region, thermal modelling results for KK1 show relatively steady cooling after a Variscan heating event due to slow exhumation, with only moderate acceleration of cooling that may be attributed to Late Cretaceous inversion (Figure 3a). KK1 and nearby OST samples have Jurassic AFT ages (168–202 Ma) and shortened MTL with standard deviations between 1.6 and 1.8. The large difference between ZHe and AFT as well as AFT and AHe ages confirm slow cooling throughout the Mesozoic and Cenozoic in this part of the HCM.

The HCF had a clear imprint on the maturity pattern created during the Variscan shortening of the HCM (Naglik et al., 2016; Narkiewicz et al., 2010; Poprawa et al., 2005) presumably providing a conduit for hydrothermal solutions circulating at that time. However, during the Late Cretaceous–earliest Palaeogene inversion, vertical displacements along the fault were probably too small to influence the maturity distribution as suggested from the thermal modelling results of samples from both sides of the fault (Figure 3b,c).

6 | CONCLUSIONS

Maturity distribution data in the pre-Permian vs. younger rocks point to a decisive role of the elevated late Palaeozoic heat flow for the HCM (cf. Narkiewicz, 2017). A late Variscan cooling event recorded by our ZHe data marks the end of an important thermal overprint presumably related to Variscan tectonics widespread in the HCM (e.g. Konon, 2006; Lamarche, Lewandowski, et al., 2003; Lamarche et al., 1999; Mizerski, 2004) and neighbouring areas (Krzywiec, Gągała, et al., 2017; Krzywiec, Mazur, et al., 2017). This event may have been caused by increased heat flow that was, at least partly, coupled with fluid circulation along the HCF (e.g. Narkiewicz et al., 2010). The increase in temperature across most of the HCM during the Mesozoic reveals subsidence of the Mid-Polish Trough and resulting burial. A final rapid cooling episode in the Late Cretaceous was caused by tectonic inversion (Krzywiec, 2002; Lamarche, Lewandowski, et al., 2003; Lamarche, Scheck, et al., 2003; Scheck-Wenderoth et al., 2008).

ACKNOWLEDGEMENTS

This research has been partially funded by the Institute of Geological Sciences, Polish Academy of Sciences and the Polish National Centre for Research and Development (NCRD) grant under the Blue Gas – Polish Shale Gas program – BG1/GAZGEOLMOD/13 (AGH No. 17.17.866660). Mariusz Paszkowski and Stanisław Mazur were supported by the National Science Centre (NCN) (grant no. UMO-2012/05/B/ST10/00521). The authors cordially thank the editors of Terra Nova (Meinert Rahn and Klaus Mezger) as well as Martin Danišík and an anonymous reviewer for their valuable input, which significantly improved the quality of the paper.

ORCID

Dariusz Botor http://orcid.org/0000-0003-0157-4885

REFERENCES

Barker, C. E., & Pawlewicz, M. J. (1994). Calculation of vitrinite reflectance from thermal histories and peak temperatures. A comparison of methods. In P. K. Mukhopadhyay & W. G. Dow (Eds.), *Vitrinite reflectance as a maturity parameter: Applications and limitations* (pp. 216–229). ACS symposium series 570. Washington, DC: American Chemical Society. https://doi.org/10.1021/symposium

Bełka, Z. (1990). Thermal maturation and burial history from conodont colour alteration data, Holy Cross Mountains, Poland. *Courier Forschungsinstitut Senckenberg*, *118*, 241–251.

Berthelsen, A. (1992). Tectonic evolution of Europe. From Precambrian to Variscan Europe. In D. Blundall, S. Freeman & S. Muller (Eds.), *A continent revealed, the European Geotraverse* (pp. 153–164). Cambridge: Cambridge University Press.

Czarnocki, J. (1919). Stratygrafia i tektonika Gór Świętokrzyskich. Prace Towarzystwa Naukowego Warszawskiego, 28, 172 pp. [in Polish]

Czarnocki, J. (1936). Przegląd stratygrafii i palaeografii dewonu dolnego Gór Świętokrzyskich. *Sprawozdania Państwowego Instytutu Geologicznego*, *8*, 129–200. [in Polish]

Czarnocki, J. (1950). Geology of the Łysa Góra Region (Święty Krzyż Mountains) in connection with the problem of iron ores at Rudki. Prace Państwowego Instytutu Geologicznego, 1, 404 pp. [in Polish, with English summary]

Dadlez, R., Kowalczewski, Z., & Znosko, J. (1994). Some key problems of the pre-Permian tectonics of Poland. *Geological Quarterly*, *38*, 169–190.

Dadlez, R., Narkiewicz, M., Stephenson, R. A., Visser, M. T. M., & van Wees, J. D. (1995). Tectonic evolution of the Mid-Polish Trough: Modelling implications and significance for central European geology. *Tectonophysics*, *252*, 179–195. https://doi.org/10.1016/0040-1951(95)00104-2

Donelick, R. A., O'Sullivan, P. B., & Ketcham, R. A. (2005). Apatite fission-track analysis. *Reviews in Mineralogy and Geochemistry*, *58*, 49–94. https://doi.org/10.2138/rmg.2005.58.3

Gągała, Ł. (2015). Late Silurian deformation in the Łysogóry Region of the Holy Cross Mountains revisited: Restoration of a progressive Caledonian unconformity in the Klonów Anticline and its implications for the kinematics of the Holy Cross Fault (central Poland). *Geological Quarterly*, *59*, 441–456.

Gradstein, F. M., Ogg, J. G., & Hilgen, F. J. (2012). On the geologic time scale. *Newsletters on Stratigraphy*, *45*, 171–188. https://doi.org/10.1127/0078-0421/2012/0020

Jaworowski, K., & Sikorska, M. (2006). Łysogóry Unit (Central Poland) versus East European Craton – Application of sedimentological data from Cambrian siliciclastic association. *Geological Quarterly*, *50*, 77–88.

Ketcham, R. A. (2005). Forward and inverse modeling of low-temperature thermochronometry data. *Reviews in Mineralogy and Geochemistry*, *58*, 275–314. https://doi.org/10.2138/rmg.2005.58.11

Ketcham, R. A., Carter, A., Donelick, R. A., Barbarand, J., & Hurford, A. J. (2007a). Improved measurement of fission track annealing in apatite using c-axis projection. *American Mineralogist*, *92*, 789–798. https://doi.org/10.2138/am.2007.2280

Ketcham, R. A., Carter, A., Donelick, R. A., Barbarand, J., & Hurford, A. J. (2007b). Improved modeling of fission track annealing in apatite. *American Mineralogist*, *92*, 799–810. https://doi.org/10.2138/am.2007.2281

Konon, A. (2006). Buckle folding in the Kielce Unit, Holy Cross Mountains, central Poland. *Acta Geologica Polonica*, *56*, 375–405.

Konon, A. (2007). Strike-slip faulting in the Kielce Unit, Holy Cross Mountains, central Poland. *Acta Geologica Polonica*, *57*, 415–441.

Kowalczewski, Z., Jaworowski, K., & Kuleta, M. (1998). Klonów Beds (uppermost Silurian-?lowermost Devonian) and the problem of Caledonian deformations in the Holy Cross Mts. *Geological Quarterly*, *42*, 341–378.

Kozłowski, W. (2003). Age, sedimentary environment and palaeogeographical position of the Late Silurian oolitic beds in the Holy Cross Mountains (Central Poland). *Acta Geologica Polonica*, *53*, 341–357.

Kozłowski, W. (2008). Lithostratigraphy and regional significance of the Nowa Słupia Group (Upper Silurian) of the Łysogóry Region (Holy Cross Mountains, Central Poland). *Acta Geologica Polonica*, *58*, 43–74.

Kozłowski, W., Domańska-Siuda, J., & Nawrocki, J. (2014). Geochemistry and petrology of the Upper Silurian greywackes from the Holy Cross Mountains (central Poland): Implications for the Caledonian history of the southern part of the Trans-European Suture Zone (TESZ). *Geological Quarterly*, *58*, 311–336.

Krzywiec, P. (2002). Mid-Polish Trough inversion – Seismic examples, main mechanisms and its relationship to the Alpine-Carpathian collision. In G. Berotti, K. Schulmann, & S. Cloetingh (Eds.), *Continental collision and the tectonosedimentary evolution of forelands* (pp. 151–165). European Geosciences Union, *Stephan Mueller Special Publication Series*, *1*.

Krzywiec, P. (2009). Devonian-Cretaceous repeated subsidence and uplift along the Teisseyre-Tornquist zone in SE Poland–Insight from seismic data interpretation. *Tectonophysics*, *475*, 142–159. https://doi.org/10.1016/j.tecto.2008.11.020

Krzywiec, P., Gągała, Ł., Mazur, S., Słonka, Ł., Kufrasa, M., Malinowski, M., . . . Golonka, J. (2017). Variscan deformation along the Teisseyre-Tornquist Zone in SE Poland: Thick-skinned structural inheritance or thin-skinned thrusting? *Tectonophysics*, *718*, 83–91. https://doi.org/10.1016/j.tecto.2017.06.008

Krzywiec, P., Gutowski, J., Walaszczyk, I., Wróbel, G., & Wybraniec, S. (2009). Tectonostratigraphic model of the Late Cretaceous inversion along the Nowe Miasto-Zawichost Fault Zone, SE Mid-Polish Trough. *Geological Quarterly*, *53*, 27–48.

Krzywiec, P., Mazur, S., Gągała, Ł., Kufrasa, M., Lewandowski, M., Malinowski, M., & Buffenmyer, V. (2017). Late Carboniferous thin-skinned compressional deformation above the SW edge of the East European craton as revealed by seismic reflection and potential field data – Correlations with the Variscides and the Appalachians. In R. D. Law, J. R. Thigpen, A. J. Merschat, & H. H. Stowell (Eds.), *Linkages and feedbacks in orogenic systems*. *Geological Society of America Memoir*, *213*, 353–372, doi:10.1130/2017.1213(14)

Kutek, J. (2001). The Polish Permo-Mesozoic Rift Basin. *Mémoires du Muséum national d'histoire naturelle*, *186*, 213–236.

Kutek, J., & Głazek, J. (1972). The Holy Cross area, central Poland, in the Alpine cycle. *Acta Geologica Polonica*, *22*, 603–651.

Lamarche, J., Lewandowski, M., Mansy, J. L., & Szulczewski, M. (2003). Partitioning pre-, syn-and post-Variscan deformation in the Holy Cross Mountains, eastern Variscan foreland. In T. McCann & A. Saintot (Eds.), *Tracing tectonic deformation using the sedimentary record*. *Geological Society*, *London*, *Special Publications*, *208*, 159–184.

Lamarche, J., Mansy, J., Bergerat, F., Averbuch, O., Hakenberg, M., Lewandowski, M., . . . Wieczorek, J. (1999). Variscan tectonics in the Holy Cross Mountains (Poland) and the role of structural inheritance during Alpine tectonics. *Tectonophysics*, *313*, 171–186. https://doi.org/10.1016/S0040-1951(99)00195-X

Lamarche, J., Scheck, M., & Lewerenz, B. (2003). Heterogeneous tectonic inversion of the Mid-Polish Trough related to crustal architecture, sedimentary patterns and structural inheritance. *Tectonophysics*, *373*, 75–92. https://doi.org/10.1016/S0040-1951(03)00285-3

Malec, J. (2015). Thermal maturity of Devonian, Carboniferous and Triassic rocks in the central part of the Małopolska Massif from conodont Colour Alteration Index. *Biuletyn Państwowego Instytutu Geologicznego*, *462*, 29–39. [in Polish, with English summary] https://doi.org/10.5604/08676143.1157484

Malec, J., Kuleta, M., & Migaszewski, Z. M. (2016). Lithologic-petrographic characterization of Silurian rocks in the Niestachów profile (Holy Cross Mountains). *Annales Societatis Geologorum Poloniae*, *86*, 85–110.

Marynowski, L. (1997). Stopień dojrzałości materii organicznej ze skał węglanowych dewonu Gór Świętokrzyskich. *Przegląd Geologiczny*, *45*, 899–903. [in Polish]

Marynowski, L. (1999). Thermal maturity of organic matter in Devonian rocks of the Holy Cross Mts. (Central Poland). *Przegląd Geologiczny*, *47*, 1125–1129. [in Polish, with English summary]

Marynowski, L., Czechowski, F., & Simoneit, B. R. T. (2001). Phenylnaphthalenes and polyphenyls in Palaeozoic source rocks of the Holy Cross Mountains, Poland. *Organic Geochemistry*, *32*, 69–85. https://doi.org/10.1016/S0146-6380(00)00150-9

Marynowski, L., Salamon, M., & Narkiewicz, M. (2002). Thermal maturity and depositional environments of organic matter in the post-Variscan succession of the Holy Cross Mountains. *Geological Quarterly*, *46*, 25–36.

Marynowski, L., & Simoneit, B. R. (2009). Widespread upper Triassic to lower Jurassic wildfire records from Poland: Evidence from charcoal and pyrolytic polycyclic aromatic hydrocarbons. *Palaios*, *24*, 785–798. https://doi.org/10.2110/palo.2009.p09-044r

Mastella, L., & Mizerski, W. (2002). Geological setting of the Łysogóry Unit (Holy Cross Mountains, Central Poland) based on analysis of the radar images. *Przegląd Geologiczny*, *50*, 767–773. [in Polish, with English summary]

Mazur, S., Scheck-Wenderoth, M., & Krzywiec, P. (2005). Different modes of the Late Cretaceous-Early Tertiary inversion in the North German and Polish basins. *International Journal of Earth Sciences*, *94*, 782–798. https://doi.org/10.1007/s00531-005-0016-z

Mizerski, W. (2004). Holy Cross Mountains in the Caledonian, Variscan and Alpine cycles – Major problems, open questions. *Przegląd Geologiczny*, *52*, 774–779. [in Polish, with English summary]

Modliński, Z., & Szymański, B. (2001). The Silurian of the Nida, Holy Cross Mts. and Radom areas, Poland – A review. *Geological Quarterly*, *45*, 435–454.

Naglik, B., Toboła, T., Natkaniec-Nowak, L., Luptáková, J., & Milovská, S. (2016). Raman spectroscopic and microthermometric studies of authigenic quartz (the Pepper Mts., Central Poland) as an indicator of fluids circulation. *Spectrochimica Acta Part A Molecular and Biomolecular Spectroscopy*, *173*, 960–964.

Narkiewicz, M. (2007). Development and inversion of Devonian and Carboniferous basins in the eastern part of the Variscan foreland (Poland). *Geological Quarterly*, *51*, 231–256.

Narkiewicz, M. (2017). Comment on a paper by Schito et al. (2017) "Thermal evolution of Palaeozoic successions of the Holy Cross Mountains (Poland)". *Marine and Petroleum Geology*, *88*, 1109–1113. https://doi.org/10.1016/j.marpetgeo.2017.02.016

Narkiewicz, M., Resak, M., Littke, R., & Marynowski, L. (2010). New constraints on the Middle Palaeozoic to Cenozoic burial and thermal history of the Holy Cross Mts. (central Poland): Results of numerical modeling. *Geologica Acta*, *8*, 189–205.

Nawrocki, J., Dunlap, J., Pecskay, Z., Krzemiński, L., Żylińska, A., Fanning, M., . . . Trela, W. (2007). Late Neoproterozoic to Early Palaeozoic palaoegeography of the Holy Cross Mountains (Central Europe): An integrated approach. *Journal of the Geological Society*, *164*, 405–423. https://doi.org/10.1144/0016-76492006-023

Poprawa, P., Żywiecki, M., & Grotek, I. (2005). Burial and thermal history of the Holy Cross Mts. area: A preliminary results of maturity modelling. *Polskie Towarzystwo Mineralogiczne-Prace Specjalne*, *26*, 251–254.

Scheck-Wenderoth, M., Krzywiec, P., Zülke, R., Maystrenko, Y., & Frizheim, N. (2008). Permian to Cretaceous tectonics. In T. McCann (Ed.), *The geology of central Europe* (pp. 999–1030). London: Geological Society of London.

Schito, A., Corrado, S., Trolese, M., Aldega, L., Caricchi, C., Cirilli, S., . . . Valentim, B. (2017). Assessment of thermal evolution of Palaeozoic successions of the Holy Cross Mountains (Poland). *Marine and Petroleum Geology*, *80*, 112–132. https://doi.org/10.1016/j.marpetgeo.2016.11.016

Smolarek, J., Marynowski, L., Spunda, K., & Trela, W. (2014). Vitrinite equivalent reflectance of Silurian black shales from the Holy Cross Mountains, Poland. *Mineralogia*, *45*, 79–96.

Środoń, J., & Trela, W. (2012). Preliminary clay mineral data on burial history of the Holy Cross Mts., Poland. *Mineralogia – Special Papers*, *39*, 93–94.

Stupnicka, E. (1988). On the nature and origin of the Holy Cross Dislocation. *Przegląd Geologiczny*, *36*, 40–46. [in Polish, with English summary]

Stupnicka, E. (1992). The significance of the Variscan orogeny in the Świętokrzyskie Mountains (Mid Polish Uplands). *Geologische Rundschau*, *81*, 561–570. https://doi.org/10.1007/BF01828615

Szaniawski, R., Konon, A., Grabowski, J., & Schnabl, P. (2011). Palaeomagnetic age constraints on folding and faulting events in Devonian carbonates of the Kielce Fold Zone (southern Holy Cross Mountains, Central Poland). *Geological Quarterly*, *55*, 223–234.

Szewczyk, J., & Gientka, D. (2009). Terrestrial heat flow density in Poland – A new approach. *Geological Quarterly*, *53*, 125–140.

Szulczewski, M. (1995). Depositional evolution of the Holy Cross Mts. (Poland) in the Devonian and Carboniferous – A review. *Geological Quarterly*, *39*, 471–488.

Szulczewski, M., Bełka, Z., & Skompski, S. (1996). The drowning of a carbonate platform: An example from the Devonian-Carboniferous of the southwestern Holy Cross Mountains, Poland. *Sedimentary Geology*, *106*, 21–49. https://doi.org/10.1016/0037-0738(95)00145-X

Znosko, J. (1996). Tectonic style of the Early Palaeozoic sequences in the Holy Cross Mountains. *Geological Quarterly*, *40*, 1–22.

SUPPORTING INFORMATION

Additional supporting information may be found online in the Supporting Information section at the end of the article.

Section SI 1. Samples and Methods.
Section SI 2. Thermal modelling.
Table SI 1. Zircon (U–Th)/He data.
Table SI 2. Apatite fission track data.
Table SI 3. Apatite (U–Th)/He data.

How to cite this article: Botor D, Anczkiewicz AA, Dunkl I, Golonka J, Paszkowski M, Mazur S. Tectonothermal history of the Holy Cross Mountains (Poland) in the light of low-temperature thermochronology. *Terra Nova*. 2018;00:1–9. https://doi.org/10.1111/ter.12336